RESEARCH ARTICLE • OPEN ACCESS

Optimal Control of an Age–Structured Pneumonia Transmission Model with Vaccination and Treatment Strategies

Dwi Lestari, Nikenasih Binatari, Eminugroho Ratna Sari

JAMBURA JOURNAL OF MATHEMATICS

Volume 8, Issue 2, Pages 159–168, August 2026

Received 12 April 2026, Revised 22 June 2026, Accepted 1 July 2026, Published 20 July 2026

To Cite this Article : D. Lestari, N. Binatari, E. R. Sari,"Optimal Control of an Age–Structured Pneumonia Transmission Model with Vaccination and Treatment Strategies ", *Jambura J. Math*, vol. 8, no. 2, pp. 159–168, 2026, *https://doi.org/10.37905/jjom.v8i2.38190*

JOURNAL INFO • JAMBURA JOURNAL OF MATHEMATICS

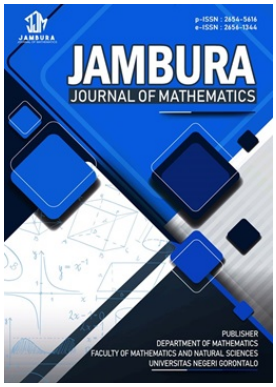

Homepage	:	http://ejurnal.ung.ac.id/index.php/jjom/index
Journal Abbreviation	:	Jambura J. Math.
Frequency	:	Biannual (February and August)
Publication Language	:	English (preferable), Indonesia
DOI	:	https://doi.org/10.37905/jjom
Online ISSN	:	2656-1344
Editor-in-Chief	:	Hasan S. Panigoro
Publisher	:	Department of Mathematics, Universitas Negeri Gorontalo
Country	:	Indonesia
OAI Address	:	http://ejurnal.ung.ac.id/index.php/jjom/oai
Google Scholar ID	:	iWLjgaUAAAAJ
Email	:	info.jjom@ung.ac.id

JAMBURA JOURNAL • FIND OUR OTHER JOURNALS

Jambura Journal of Biomathematics

Jambura Journal of Mathematics Education

Jambura Journal of Probability and Statistics

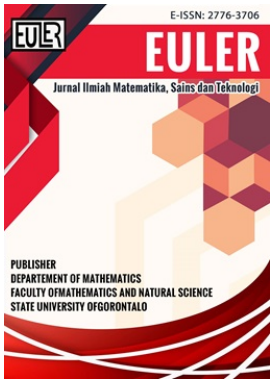

EULER : Jurnal Ilmiah Matematika, Sains, dan Teknologi

Jambura Journal of Mathematics, Volume 8, Issue 2, Pages 159–168, August 2026 https://doi.org/10.37905/jjom.v8i2.38190

Research Article

Check for updates

Optimal Control of an Age–Structured Pneumonia Transmission Model with Vaccination and Treatment Strategies

Dwi Lestari[1,*], **Nikenasih Binatari**[1], **Eminugroho Ratna Sari**[1]

[1]*Department of Mathematics Education, Universitas Negeri Yogyakarta, Yogyakarta 55281, Indonesia*

ARTICLE HISTORY
Received 12 April 2026
Revised 22 June 2026
Accepted 1 July 2026
Published 20 July 2026

KEYWORDS
Optimal control
Pneumonia
Pontryagin's maximum principle
children
elderly

ABSTRACT. *This research aims to apply optimal control to model the pneumonia disease using a system of ordinary differential equations. We developed based on the SIR pneumonia epidemic model. We divided the population into two groups: children and the elderly. The optimal controls illustrate the effectiveness of vaccination and treatment in preventing new infections among both children and the elderly. The Pontryagin's maximum principle is used to define the optimal controls, and the resulting optimality system is formulated and solved numerically. Numerical simulations have been performed. It was found that combining vaccination and treatment effectively reduces the number of pneumonia infections. In fact, when we change the cost scenario, we see changes in the control variables. This study supports the joint implementation of vaccination and therapeutic interventions to control pneumonia transmission among children and the elderly, particularly in developing countries where economic limitations, inadequate infrastructure, and distribution barriers restrict vaccine access.*

1. Introduction

Pneumonia is a lung infection that causes inflammation of the air sacs, which can lead to oxygen deprivation, difficulty breathing, and even death [1, 2]. Pneumonia is caused by bacteria, viruses, fungi, or parasites; among these, bacteria are the leading cause of community-acquired pneumonia (CAP) worldwide. The most common bacteria causing CAP are Streptococcus pneumoniae [3, 4]. In addition, several direct factors can also trigger pneumonia, such as smoking, chronic heart disease, diabetes mellitus, weakened respiratory structures, and decreased level of consciousness. Pneumonia is transmitted through multiple pathways, primarily via inhalation of airborne droplets released during coughing or sneezing that contain infectious agents such as bacteria, viruses, or fungi [3].

Although pneumonia can affect individuals of all ages, children under five, adults over sixty-five, and people with underlying medical conditions or compromised immune systems are at the highest risk [5]. Pneumonia is a major infectious disease causing death in children, killing approximately 700,000 children globally each year. It corresponding to a worldwide rate of 1,400 cases per 100,000 children [6]. During the 2017–2021 period, the mean annual number of pneumonia cases in Jakarta was 7,267, reaching a maximum of 8,804 cases in 2019. Additionally, pneumonia caused an average of 25 deaths per year, with the highest mortality recorded in 2020 at 39 deaths [7].

Pneumonia data in children under five in the Special Region of Yogyakarta (DIY) over the past seven years (2018-2024) were reported by various government health service facilities in the region. These data indicate that the percentage of pneumonia cases detected in children under five in 2024 was 86%. This means that cases of pneumonia in children under five experienced a significant increase compared to 2023 (61%). Furthermore, the number of new cases has increased annually, with the highest number recorded in 2023, with 16.256 new cases [8].

GTWR has proven effective for analyzing dynamic data with Based on [5], Preventive measures for pneumonia encompass immunization, adequate nutrition, pharmacological treatment, and environmental management. Available pneumonia vaccines include the pneumococcal conjugate vaccine (PCV), pneumococcal polysaccharide vaccine (PPV), and the Haemophilus influenzae type b conjugate vaccine (Hib CV) [9]. According to the Global Vaccine Action Plan 2011–2020 (GVAP), reports indicate that in middle-income countries not supported by the Global Alliance for Vaccines and Immunization (Gavi). The cost of vaccines remains a major barrier to immunization programs; consequently, the affordability of vaccines in developing countries remains problematic [10]. In addition, Pneumonia is generally managed with antibiotic therapy, with amoxicillin being the most commonly recommended oral medication because of its effectiveness [5]. Pneumonia treatment has the potential to save over 600,000 lives each year [11].

Numerous mathematical studies have investigated the dynamics of pneumonia transmission [12]. For instance, A mathematical model was developed to describe pneumonia dynamics involving carriers, with a focus on the impact of carriers on disease prevalence [13]. The findings indicated that transmission between carriers and infected individuals is a key parameter; however, the model did not incorporate intervention strategies such as medication, adequate nutrition, or vaccination.

*Corresponding Author.

Email : *dwilestari@uny.ac.id* (Dwi Lestari)
Homepage : http://ejurnal.ung.ac.id/index.php/jjom/index / E-ISSN : 2656-1344

Mathematical models of optimal control problems [14] can be analyzed using Pontryagin's Maximum Principle. Research by [4] found that implementing treatment early in infected population is necessary to avoid more significant pneumonia outbreaks in the long term. Therefore, this study developed a mathematical model of the dynamics of pneumonia spread in children under 5 years of age and adults over 65 years of age, implementing controls in the form of vaccines and medication. The mathematical model developed was a modification of the model from [3]. Vaccines are administered to children and the elderly, and medication is administered to both children and adults. Implementing optimal control is expected to be a strategy for preventing the spread of pneumonia and minimizing the costs of vaccines and medication.

Therefore, the novelty of this study can be summarized as follows: (1) A new mathematical model which modifies and extends the work of [3] by adding control variables and cost functions associated with vaccination and medication; (2) Two optimal control strategies are introduced, namely vaccination for children and the elderly, and medication for both children and adults, to reflect realistic intervention efforts; (3) While Pontryagin's Maximum Principle is a well-established analytical tool, its novel application in this study lies in optimizing age-structured pneumonia dynamics with dual controls vaccination and medication applied simultaneously to distinct age groups. This approach allows the derivation of optimal strategies that minimize both infection levels and total intervention costs under realistic demographic settings. Thus, the aim of this study is to apply optimal control to a model of pneumonia disease using a system of ordinary differential equations. Furthermore, the model is solved with optimal control using the Pontryagin's Minimum Principle.

2. Methods

This study was carried out through the following steps:

1. Conducting a literature review to obtain reference materials for analyzing a pneumonia model that incorporates vaccination and treatment, as well as optimal control. At this stage, relevant sources related to the research topic were used.
2. Formulating assumptions, determining parameters, and constructing the model. In this phase, the assumptions underlying the study were established and the model parameters were identified based on these assumptions.
3. Determining the equilibrium points and the basic reproduction number of the model. Here, the definition of equilibrium points was applied to identify the types of equilibria produced by the model.
4. Analyzing the model under optimal control, where vaccination and treatment were considered as the control variables for pneumonia.
5. Performing simulations and interpreting the model. Parameter values were selected based on journal references or assumptions, and simulations were conducted using Python software. The numerical simulations aimed to verify the consistency between analytical results and computational outcomes by solving the model with and without control. Finally, the results were interpreted.

3. Results and Discussion

3.1. Mathematical Modeling

This study extends the model proposed by [3] by introducing additional control variables to enhance pneumonia prevention and treatment strategies. Before presenting the extended model, we first describe in detail the original mathematical model developed by [3] to provide a clear foundation for the modifications introduced in this work.

In the original model by [3], the total population is divided into two main groups children and the elderly to reflect the age-structured dynamics of pneumonia transmission. Each group is further categorized into three epidemiological classes: susceptible, infected, and recovered individuals.

Children and the elderly enter the susceptible population at rates Λ and Π, respectively. A susceptible individual gets pneumonia upon contact with an infectious person, either a child or an adult. The force of infection is given by $\lambda_i = \beta_i(I_c + I_e)$, where $i = c, e$ represents children and the elderly, and β_i denotes their respective transmission rates. The parameter $\alpha_i = 1 - \alpha_j$, for $j = 1, 2$ represents the rate of proper nutrition among children and the elderly, with $\alpha_j \in [0, 1]$. Adequate nutrition strengthens the immune system and thus reduces the risk of infection. In this research, the rate of proper nutrition change into vaccine rate.

Susceptible children become infected at a rate $\alpha_c\lambda_c$, where $\alpha_c = (1 - \alpha_1)$, and α_1 denotes the rate of vaccine for children. Infected children may decrease the infected class either through disease-induced death at a rate ω_c or become recovered at a rate η_c, which represents the treatment rate. Since pneumonia does not confer permanent immunity, recovered children lose temporary immunity at a rate γ_c and return to the susceptible class.

Similarly, susceptible adults move to the infected class at an incidence rate $\alpha_e\lambda_e$, where $\alpha_e = (1 - \alpha_2)$, and α_2 represents the rate of vaccine for adults. Infected adults may die from the disease at a rate ω_e or recover at a rate η_e, that represents the treatment rate for adults. Recovered adults are assumed to acquire only temporary immunity, which wanes at a rate γ_e, leading them back to the susceptible class. Finally, it is assumed that any individual can die naturally at a rate μ. The pneumonia transmission model formulated by [3] is described as follows.

$$\begin{aligned}
\frac{dS_c}{dt} &= \Lambda + \gamma_c R_c - (\mu + \alpha_c\lambda_c)S_c,\\
\frac{dI_c}{dt} &= \alpha_c\lambda_c S_c - (\mu + \omega_c + \eta_c)I_c,\\
\frac{dR_c}{dt} &= \eta_c I_c - (\mu + \gamma_c)R_c,\\
\frac{dS_e}{dt} &= \pi + \gamma_e R_e - (\mu + \alpha_e\lambda_e)S_e,\\
\frac{dI_e}{dt} &= \alpha_e\lambda_e S_e - (\mu + \omega_e + \eta_e)I_e,\\
\frac{dR_e}{dt} &= \eta_e I_e - (\mu + \gamma_e)R_e,
\end{aligned} \tag{1}$$

where

$$\begin{aligned}
\lambda_c &= \beta_c(I_c + I_e),\\
\lambda_e &= \beta_e(I_c + I_e),\\
\alpha_c &= 1 - \alpha_1,\\
\alpha_e &= 1 - \alpha_2.
\end{aligned}$$

The variable and parameter notations are presented in Table 1 and Table 2, respectively.

Table 1. The variable notation.

Variable notation	Description	Value
$S_c(t)$	Susceptible population of children at time t	≥ 0
$I_c(t)$	Infected population of children at time t	≥ 0
$R_c(t)$	Recovered population of children at time t	≥ 0
$S_e(t)$	Susceptible population of elders at time t	≥ 0
$I_e(t)$	Infected population of elders at time t	≥ 0
$R_e(t)$	Recovered population of elders at time t	≥ 0

Table 2. The parameter.

Notation	Description	Value	Ref.
Λ	Children recruitment rate	0.05	[3]
π	Elders recruitment rate	0.0381	[3]
μ	Natural death rate	0.02	[3]
β_c	Transmission rate for children	0.5445	[3]
β_e	Transmission rate for elders	0.25	[3]
α_1	Rate of vaccine in children	[0,1]	[3]
α_2	Rate of vaccine in elderly	[0,1]	[3]
ω_c	Disease induced death rate for children	0.33	[3]
ω_e	Disease induced death rate for elders	0.2	[3]
η_c	Recovery rate for children due to treatment	0.08	[3]
η_e	Recovery rate for elderly due to treatment	0.06	[3]
γ_c	Rate of recovered children to become susceptible	0.0241	[3]
γ_e	Rate of recovered elders to become susceptible	0.00833	[3]

To ensure that the model solution accurately represents the real population, it is necessary to establish the non-negativity of the solutions to system (1). Since negative population values are not feasible, the non-negativity of these solutions is proven in Theorem 1.

Theorem 1. *If the initial conditions* $\{S_c(0) \geq 0, I_c(0) \geq 0, R_c(0) \geq 0, S_e(0) \geq 0, I_e(0) \geq 0, R_e(0) \geq 0\} \in \mathbb{R}^6$ *then the solutions* $\{S_c(t), I_c(t), R_c(t), S_e(t), I_e(t), R_e(t)\}$ *of the system (1) are non-negative for all* $t \geq 0$.

Proof. The detailed proof is analog to [3]. ■

In the following section, we analyze the equilibrium points of system (1) along with their stability properties. In general, two types of equilibria are identified: the disease-free and endemic equilibria. The local stability of these equilibria is investigated using the basic reproduction number.

3.2. Equilibrium Points

The mathematical model describing the spread of pneumonia in toddlers and elders reaches an equilibrium state when each equation in system (1) equal to zero.

Theorem 2. *The following statements hold:*

(a) If $I_c = I_e = 0$ *then the system (1) has a disease-free equilibrium point, namely:*

$$E_0 = (S_c, I_c, R_c, S_e, I_e, R_e) = (S_c^*, 0, 0, S_e^*, 0, 0)$$

with $S_c^* = \frac{\Lambda}{\mu}$ *and* $S_e^* = \frac{\pi}{\mu}$.

(b) If $I_c \neq I_e \neq 0$ *then the system (1) has an endemic equilibrium point, yaitu:*

$$E_1 = (S_c, I_c, R_c, S_e, I_e, R_e) = (S_c^*, I_c^*, R_c^*, S_e^*, I_e^*, R_e^*)$$

with:

$$\begin{aligned}
S_c^* &= \frac{\Lambda(\mu+\gamma_c)+\gamma_c(\eta_c I_c^*)}{(\mu+\gamma_c)(\mu+\alpha_c\lambda_c)},\\
I_c^* &= \frac{(\alpha_c\lambda_c^*\Lambda)(\mu+\gamma_c)}{(\mu+\gamma_c)(\mu+\alpha_c\lambda_c^*)(\mu+\omega_c+\eta_c)-\alpha_c\lambda_c^*\gamma_c\eta_c},\\
R_c^* &= \frac{\eta_c I_c^*}{\mu+\gamma_c},\\
S_e^* &= \frac{\pi(\mu+\gamma_e)+\gamma_e\eta_e I_e^*}{(\mu+\gamma_e)(\mu+\alpha_e\lambda_e)},\\
I_e^* &= \frac{(\alpha_e\lambda_e^*\pi)(\mu+\gamma_e)}{(\mu+\gamma_e)(\mu+\alpha_e\lambda_e^*)(\mu+\omega_e+\eta_e)-\alpha_e\lambda_e^*\gamma_e\eta_e},\\
R_e^* &= \frac{\eta_e I_e^*}{\mu+\gamma_e},\\
\lambda_c^* &= \beta_c(I_c^*+I_e^*),\\
\lambda_e^* &= \beta_e(I_c^*+I_e^*).
\end{aligned}$$

Proof. If $I_c = I_e = 0$ substituted to third and sixth equation of system (1), obtained $R_c = 0$ and $R_e = 0$. As a result, it is obtained $S_c = \frac{\Lambda}{\mu}$ and $S_e = \frac{\pi}{\mu}$, such that the point of disease-free equilibrium is $E_0 = (S_c^*, I_c^*, R_c^*, S_e^*, I_e^*, R_e^*) = \left(\frac{\Lambda}{\mu}, 0, 0, \frac{\pi}{\mu}, 0, 0\right)$. Furthermore, if $I_c \neq I_e \neq 0$, then analogously, an endemic equilibrium point will be obtained. ■

3.3. Basic Reproduction Number

In epidemic models of disease transmission, the basic reproduction number is used as a key parameter to assess the potential for disease outbreaks in a population. The basic reproduction number R_0 represents the average number of individuals infected by a single infected person. Disease transmission occurs when $R_0 > 1$, since, on average, an infected individual generates more than one new infection. Conversely, if $R_0 < 1$, transmission does not persist because each infected individual

infects fewer than one new person on average [15].

Basic reproductive numbers R_0 of the system (1) will be found by using the Next Generation Matrix. This matrix is formed based on the subpopulation that caused the infection. In this model, the cause of infection is an infected subpopulation of toddlers I_c and the elderly subpopulation is infected I_e so that obtained:

$$\frac{dI_c}{dt} = \alpha_c\lambda_c S_c - (\mu + \omega_c + \eta_c)I_c,$$
$$\frac{dI_e}{dt} = \alpha_e\lambda_e S_e - (\mu + \omega_e + \eta_e)I_e,$$

with

$$\lambda_c = \beta_c(I_c + I_e),$$
$$\lambda_e = \beta_e(I_c + I_e),$$
$$\alpha_c = 1 - \alpha_1,$$
$$\alpha_e = 1 - \alpha_2.$$

Analogue using the steps in [16], the formula of basic reproduction number of system (1) is given by

$$R_0 = \frac{\alpha_c\beta_c\Lambda}{\mu(\mu + \omega_c + \eta_c)} + \frac{\alpha_e\beta_e\pi}{\mu(\mu + \omega_e + \eta_e)}.$$

3.4. The Stability Analysis

Local stability can be analyzed by linearizing the model around its equilibrium points using a Taylor series expansion. An equilibrium point is considered stable if the real parts of the characteristic roots are negative or equal to zero [17].

Furthermore, the stability analysis around the disease-free equilibrium point is expressed in the following Theorem 3.

Theorem 3. *The disease-free equilibrium point (E_0) satisfies the following properties:*

i. If $R_0 < 1$, then the disease-free equilibrium point (E_0) is locally asymptotically stable.

ii. If $R_0 > 1$, then the disease-free equilibrium point (E_0) is unstable.

Proof. The linearization result of the system (1) is a Jacobian matrix:

$$J = \begin{bmatrix} \frac{\partial f_1}{\partial S_c} & \frac{\partial f_1}{\partial I_c} & \frac{df_1}{dR_c} & \frac{\partial f_1}{\partial S_e} & \frac{\partial f_1}{\partial I_e} & \frac{\partial f_1}{\partial R_e} \\ \frac{\partial f_2}{\partial S_c} & \frac{\partial f_2}{\partial I_c} & \frac{df_2}{dR_c} & \frac{\partial f_2}{\partial S_e} & \frac{\partial f_2}{\partial I_e} & \frac{\partial f_2}{\partial R_e} \\ \frac{\partial f_3}{\partial S_c} & \frac{\partial f_3}{\partial I_c} & \frac{df_3}{dR_c} & \frac{\partial f_3}{\partial S_e} & \frac{\partial f_3}{\partial I_e} & \frac{\partial f_3}{\partial R_e} \\ \frac{\partial f_4}{\partial S_c} & \frac{\partial f_4}{\partial I_c} & \frac{df_4}{dR_c} & \frac{\partial f_4}{\partial S_e} & \frac{\partial f_4}{\partial I_e} & \frac{\partial f_4}{\partial R_e} \\ \frac{\partial f_5}{\partial S_c} & \frac{\partial f_5}{\partial I_c} & \frac{df_5}{dR_c} & \frac{\partial f_5}{\partial S_e} & \frac{\partial f_5}{\partial I_e} & \frac{\partial f_5}{\partial R_e} \\ \frac{\partial f_6}{\partial S_c} & \frac{\partial f_6}{\partial I_c} & \frac{df_6}{dR_c} & \frac{\partial f_6}{\partial S_e} & \frac{\partial f_6}{\partial I_e} & \frac{\partial f_6}{\partial R_e} \end{bmatrix},$$

so that

$$J = \begin{bmatrix} -(\mu+\alpha_c\lambda_c) & -\alpha_c\beta_c S_c & \gamma_c & 0 & -\alpha_c\beta_c S_c & 0 \\ \alpha_c\lambda_c & \alpha_c\beta_c S_c - (\mu+\omega_c+\eta_c) & 0 & 0 & \alpha_c\beta_c S_c & 0 \\ 0 & \eta_c & -(\mu+\gamma_c) & 0 & 0 & 0 \\ 0 & -\alpha_e\beta_e S_e & 0 & -(\mu+\alpha_e\lambda_e) & -\alpha_e\beta_e S_e & \gamma_e \\ 0 & \alpha_e\beta_e S_e & 0 & \alpha_e\lambda_e & \alpha_e\beta_e S_e - (\mu+\omega_e+\eta_e) & 0 \\ 0 & 0 & 0 & 0 & \eta_e & -(\mu+\gamma_e) \end{bmatrix}.$$

By subtituting E_0, then obtained

$$J(E_0) = \begin{bmatrix} -\mu & -\frac{\alpha_c\beta_c\Lambda}{\mu} & \gamma_c & 0 & -\frac{\alpha_c\beta_c\Lambda}{\mu} & 0 \\ 0 & \frac{\alpha_c\beta_c\Lambda}{\mu} - (\mu+\omega_c+\eta_c) & 0 & 0 & \frac{\alpha_c\beta_c\Lambda}{\mu} & 0 \\ 0 & \eta_c & -(\mu+\gamma_c) & 0 & 0 & 0 \\ 0 & -\frac{\alpha_e\beta_e\pi}{\mu} & 0 & -\mu & -\frac{\alpha_e\beta_e\pi}{\mu} & \gamma_e \\ 0 & \frac{\alpha_e\beta_e\pi}{\mu} & 0 & 0 & \frac{\alpha_e\beta_e\pi}{\mu} - (\mu+\omega_e+\eta_e) & 0 \\ 0 & 0 & 0 & 0 & \eta_e & -(\mu+\gamma_e) \end{bmatrix}.$$

If λ are eigenvalues and I is the identity matrix, then the eigen value of the matrix $J(E_0)$ can be determined by:

$$\det(\lambda I - J(E_0)) = 0.$$

By using Routh-Hurwitz criterion, the real part of the eigen values $\lambda_1, \lambda_2, \lambda_3, \lambda_4, \lambda_5, \lambda_6 < 0$, then $E_0 = \left(\frac{\Lambda}{\mu}, 0, 0, \frac{\pi}{\mu}, 0, 0\right)$ is locally asymptotically stable. ■

3.5. A Sensitivity Analysis

A sensitivity analysis of the SIR (Susceptible, Infectious, and Recovered) epidemic model is performed to identify which parameters most strongly influence the basic reproduction number [18].

The normalized sensitivity index, obtained by differentiating R_0 with respect to the parameters s_i for $i = 1, 2, \ldots, n$ can be expressed as follows

$$\Upsilon_{s_i}^{R_0} = \frac{\partial R_0}{\partial s_i} \times \frac{s_i}{R_0}.$$

The sensitivity index R_0 depends on the differentiation of the parameters. Suppose that the parameter values are given in Table 2. Based on the parameter values in Table 2, this value produces $R_0 = 4.866 > 1$ and a sensitivity index of R_0 is obtained as shown in the Table 3.

Based on the signs of the sensitivity indices in the Table 3, the value of R_0 increases with $\Lambda, \pi, \beta_c, \beta_e, \alpha_c$, and α_e, whereas it decreases with $\mu, \omega_c, \omega_e, \eta_c$, and η_e. In contrast, the parameter γ_c and γ_e have no effect on R_0. The most sensitive parameter is identified by the largest sensitivity index. In this case, Λ, β_c, and α_c are the most sensitive parameter, such that a 10% increase (or decrease) in those parameters leads to a 6.5% increase (or decrease) in R_0. Furthermore, an increase (or decrease) in $\mu, \omega_c, \omega_e, \eta_c$, and η_e leads to a reduction (or raise) in R_0. In contrast, variations in the parameter representing individuals (children and elder) who recovered to become susceptible do not affect the value of R_0.

Table 3. A Sensitivity analysis.

Notation	Description
Λ	0.6504960000
π	0.3495040000
μ	-1.055220199
β_c	0.6504960000
β_e	0.3495040000
$\alpha_c = 1 - \alpha_1$	0.6504960000
$\alpha_e = 1 - \alpha_2$	0.3495040000
ω_c	-0.4992178605
ω_e	-0.2496457142
η_c	-0.1210225116
η_e	-0.07489371429
γ_c	0
γ_e	0

3.6. Bifurcation Analysis

It has been shown that by using a next-generation matrix, the basic reproduction number is obtained as in section 3.3. Furthermore, it is shown that transcritical bifurcation occurs at the basic reproduction number. Next, this paper will show an analysis of the occurrence of Hopf bifurcation, which is a condition where outbreaks occur repeatedly. Hopf bifurcation occurs by observing the existence of pure imaginary eigenvalues in the characteristic equation around the endemic equilibrium point.

3.6.1. The endemic equilibrium point

The endemic equilibrium point denoted by $E^*(S_c^*, I_c^*, R_c^*, S_e^*, I_e^*, R_e^*)$ is the situation where an infectious disease persists in a population at a constant, non-zero level over time, $I_c^* > 0, I_e^* > 0$. By equating the right-hand side of the system (1) into zero, it is obtained

$$S_c^* = \frac{\mu + \omega_c + \eta_c}{\alpha_c \beta_c} \frac{I_c^*}{I_c^* + I_e^*}, R_c^* = \frac{\eta_c}{\mu + \gamma_c} I_c^*, S_e^* = \frac{\mu + \omega_e + \eta_e}{\alpha_e \lambda_e},$$

$$R_e^* = \frac{\eta_e}{\mu + \gamma_e} I_e^*,$$

$$\Lambda = (\mu + \omega_c + \eta_c) \frac{I_c^*}{I_c^* + I_e^*} \left(1 + \frac{\mu}{\alpha_c \beta_c}\right) - \frac{\gamma_c \eta_c}{\mu + \gamma_c} I_c^*,$$

$$\pi = (\mu + \omega_e + \eta_e) \frac{I_e^*}{I_c^* + I_e^*} \left(1 + \frac{\mu}{\alpha_e \beta_e}\right) - \frac{\gamma_e \eta_e}{\mu + \gamma_e} I_e^*.$$

The corresponding Jacobian matrix is given by

$$J(E^*) = \begin{bmatrix} a_{11} & -\alpha_c\beta_c S_c^* & \gamma_c & 0 & -\alpha_c\beta_c S_c^* & 0 \\ a_{21} & a_{22} & 0 & 0 & \alpha_c\beta_c S_c^* & 0 \\ 0 & \eta_c & -(\mu+\gamma_c) & 0 & 0 & 0 \\ 0 & -\alpha_e\beta_e S_e^* & 0 & a_{44} & -\alpha_e\beta_e S_e^* & \gamma_e \\ 0 & \alpha_e\beta_e S_e^* & 0 & a_{54} & a_{55} & 0 \\ 0 & 0 & 0 & 0 & \eta_e & -(\mu+\gamma_e) \end{bmatrix},$$

where $a_{11} = -\mu - \alpha_c\beta_c(I_c^* + I_e^*)$, $a_{21} = \alpha_c\beta_c(I_c^* + I_e^*)$, $a_{22} = \alpha_c\beta_c S_c^* - (\mu + \omega_c + \eta_c)$ $a_{44} = -\mu - \alpha_e\beta_e(I_c^* + I_e^*)$, $a_{54} = \alpha_e\beta_e(I_c^* + I_e^*)$ and $a_{55} = \alpha_e\beta_e S_e^* - (\mu + \omega_e + \eta_e)$.
Hence, the characteristic equation is given by

$$(\lambda + (\mu + \gamma_c))(\lambda + \mu + \gamma_e)(\lambda^4 + A_3\lambda^3 + A_2\lambda^2 + A_1\lambda + A_0) = 0,$$

where
$A_3 = 2\mu + \omega_c + \omega_e + \eta_c + \eta_e + \alpha_c\beta_c(I_c^* + I_e^*) + \alpha_e\beta_e(I_c^* + I_e^*)$,
$A_2 = (\mu + \alpha_c\beta_c I_c^*)(\mu + \omega_c + \eta_c - \alpha_c\beta_c S_c^*) + (\mu + \alpha_e\beta_e[I_c^* + I_e^*])(\mu + \omega_e + \eta_e - \alpha_e\beta_e S_e^*) + (\mu + \alpha_c\beta_c[I_c^* + I_e^*])(\mu + \alpha_e\beta_e[I_c^* + I_e^*]) + \alpha_c\beta_c\alpha_e\beta_e S_c^* S_e^*$.

As can be seen that the first two eigen values are always real negative. Due to the existence of endemic equilibrium point, all coefficients are positive. These imply that the purely imaginary roots will never exist. Hence, we can concluded that the Hopf bifurcation cannot occur.

3.7. Optimal Control Model

This research develops system (1) with a vaccine intervention parameter (α). Furthermore, vaccine control measures are provided for both the child and elderly populations, as well as medication control measures for both populations. The control variables appear in the infected child and adult compartments, since these groups play a crucial role in maintaining the transmission chain of pneumonia. Applying control measures to these compartments reflects realistic intervention strategies, where vaccination and treatment directly reduce the infection rate and accelerate recovery, thereby lowering the overall disease prevalence. Therefore, the control model is as follows:

$$\begin{aligned} \frac{dS_c}{dt} &= \Lambda + \gamma_c R_c - (\mu + \alpha_c\lambda_c) S_c, \\ \frac{dI_c}{dt} &= \alpha_c\lambda_c S_c - (\mu + \omega_c + \eta_c + u_2(t)) I_c, \\ \frac{dR_c}{dt} &= (\eta_c + u_2(t)) I_c - (\mu + \gamma_c) R_c, \\ \frac{dS_e}{dt} &= \pi + \gamma_e R_e - (\mu + \alpha_e\lambda_e) S_e, \\ \frac{dI_e}{dt} &= \alpha_e\lambda_e S_e - (\mu + \eta_e + \omega_e) I_e - u_2(t) I_e, \\ \frac{dR_e}{dt} &= (\eta_e + u_2(t)) I_e - (\mu + \gamma_e) R_e, \end{aligned} \tag{2}$$

where

$$\begin{aligned} \lambda_c &= \beta_c(I_c + I_e), \\ \lambda_e &= \beta_e(I_c + I_e), \\ \alpha_c &= 1 - u_1(t), \\ \alpha_e &= 1 - u_1(t). \end{aligned}$$

u_1 is the control variable for vaccine administration to children and the elderly, while u_2 is the treatment variable for children and the elderly, where u_1 and u_2 depend on t, i.e., $u_1(t)$ and $u_2(t)$. We assume that the control variable of vaccine and treatment are same for children and the elderly.

According to the proposed system (2), the optimal control of this problem is to minimise the number of infected individuals for both children and the elderly while reducing the overall cost of controlling the disease dynamics, $u_1(t)$ and $u_2(t)$. The

objective function can be written as follows:

$$J(u_1(t), u_2(t)) = \int_0^{t_f} c_1 I_c(t) + c_2 I_e(t) + \frac{1}{2} c_3 u_1^2(t) + \frac{1}{2} c_4 u_2^2(t)\, dt, \tag{3}$$

where the positive constants c_1 and c_2 represent the weight associated with the infected individuals in linear terms, $c_1 I_c(t) + c_2 I_e(t)$. Meanwhile, the other positive constants, c_3 and c_4, are the balancing terms for the quadratic controls, $\frac{1}{2} c_3 u_1^2(t) + \frac{1}{2} c_4 u_2^2(t)$. In other words, our goal is to find u_1^* and u_2^* such that

$$J(u_1^*, u_2^*) = \min\{J(u_1(t), u_2(t) : u_1(t), u_2(t) \in U\}, \tag{4}$$

where U is a set of Lebesgue integrable functions on the interval $[0, \infty)$ with $0 \le u_1(t) \le 1$, $0 \le u_2(t) \le 1$. The optimal control variable can then be determined in the following theorem.

The existence analysis of the control is carried out to demonstrate and substantiate that the formulated control variables yield beneficial effects and provide deeper insight. The existence of an optimal control pair can be established using a result by [19].

Theorem 4. *There is an optimal control $(u_1^*(t), u_2^*(t))$ within the system (2), such that the following condition is satisfied*

$$J(u_1^*(t), u_2^*(t)) = \min_{u \in U} J(u_1(t), u_2(t)).$$

The optimal control variable is then characterized in the following Theorem 5.

Theorem 5. *If u_1^* and u_2^* are the optimal control that minimize eq. (3) with system (2) as the constraint, then there exist costate variables $p_1, p_2, \ldots, p_6$ such that*

$$\begin{aligned}
\dot{p}_1 &= -\frac{\partial H}{\partial S_c} = -(-p_1(\mu + \alpha_c\lambda_c) + \alpha_c\lambda_c p_2) \\
&= p_1(\mu + \alpha_c\lambda_c) - \alpha_c\lambda_c p_2, \\
\dot{p}_2 &= -\frac{\partial H}{\partial I_c} = -(c_1 - p_1\alpha_c\beta_c + p_2\alpha_c\beta_c \\
&\quad - (\mu + \omega_c + \eta_c + u_2)p_2 + (\eta_c + u_2)p_3) \\
&= -c_1 + (p_1 - p_2)\alpha_c\beta_c + (\mu + \omega_c + \eta_c + u_2)p_2 - (\eta_c + u_2)p_3, \\
\dot{p}_3 &= -\frac{\partial H}{\partial R_c} = -(\gamma_c p_1 - (\mu + \gamma_c)p_3) \\
&= -\gamma_c p_1 + (\mu + \gamma_c)p_3, \\
\dot{p}_4 &= -\frac{\partial H}{\partial S_e} = -(-(\mu + \alpha_e\lambda_e)p_4 + \alpha_e\lambda_e p_5) \\
&= (\mu + \alpha_e\lambda_e)p_4 - \alpha_e\lambda_e p_5, \\
\dot{p}_5 &= -\frac{\partial H}{\partial I_e} = -(c_2 - p_4\alpha_e\beta_e + p_5\alpha_e\beta_e \\
&\quad - (\mu + \eta_e + \omega_e)p_5 - u_2 p_5 + (\eta_e + u_2)p_6) \\
&= -c_2 + (p_4 - p_5)\alpha_e\beta_e + (\mu + \eta_e + \omega_e)p_5 + u_2 p_5 - (\eta_e + u_2)p_6, \\
\dot{p}_6 &= -\frac{\partial H}{\partial R_e} = -(\gamma_e p_4 - (\mu + \gamma_e)p_6) \\
&= -\gamma_e p_4 + (\mu + \gamma_e)p_6,
\end{aligned}$$

with the transversality conditions: $p_1(t_f) = 0, p_2(t_f) = 0, p_3(t_f) = 0, p_4(t_f) = 0, p_5(t_f) = 0, p_6(t_f) = 0.$

$$u_1^* = \min\left\{\max\left\{0, \frac{(p_2 - p_1)\lambda_c S_c + (p_5 - p_4)\lambda_e S_e}{c_3}\right\}, 1\right\},$$

and

$$u_2^* = \min\left\{\max\left\{0, \frac{(p_2 - p_3)I_c + (p_5 - p_6)I_e}{c_4}\right\}, 1\right\}.$$

Proof. To solve the optimal control problem, we transform the constrained optimisation problem into an unconstrained optimisation problem. This step uses the Hamiltonian function, defined as in Eq. (5).

$$\begin{aligned}
H = {} & c_1 I_c + c_2 I_e + \frac{1}{2} c_3 u_1^2 + \frac{1}{2} c_4 u_2^2 \\
& + p_1\left[\Lambda + \gamma_c R_c - (\mu + \alpha_c\lambda_c)S_c\right] \\
& + p_2\left[\alpha_c\lambda_c S_c - (\mu + \omega_c + \eta_c + u_2)I_c\right] \\
& + p_3\left[(\eta_c + u_2)I_c - (\mu + \gamma_c)R_c\right] \\
& + p_4\left[\pi + \gamma_e R_e - (\mu + \alpha_e\lambda_e)S_e\right] \\
& + p_5\left[\alpha_e\lambda_e S_e - (\mu + \eta_e + \omega_e)I_e - u_2 I_e\right] \\
& + p_6\left[(\eta_e + u_2)I_e - (\mu + \gamma_e)R_e\right].
\end{aligned} \tag{5}$$

Here are the adjoint functions. By applying Pontryagin's Maximum Principle, there exist adjoint functions satisfying the adjoint system as given system 6,

$$\begin{aligned}
\dot{p}_1 &= -\frac{\partial H}{\partial S_c} = -(-p_1(\mu + \alpha_c\lambda_c) + \alpha_c\lambda_c p_2) \\
&= p_1(\mu + \alpha_c\lambda_c) - \alpha_c\lambda_c p_2, \\
\dot{p}_2 &= -\frac{\partial H}{\partial I_c} = -\big(c_1 - p_1\alpha_c\beta_c + p_2\alpha_c\beta_c \\
&\quad - (\mu + \omega_c + \eta_c + u_2)p_2 + (\eta_c + u_2)p_3\big) \\
&= -c_1 + (p_1 - p_2)\alpha_c\beta_c \\
&\quad + (\mu + \omega_c + \eta_c + u_2)p_2 - (\eta_c + u_2)p_3, \\
\dot{p}_3 &= -\frac{\partial H}{\partial R_c} = -(\gamma_c p_1 - (\mu + \gamma_c)p_3) \\
&= -\gamma_c p_1 + (\mu + \gamma_c)p_3, \\
\dot{p}_4 &= -\frac{\partial H}{\partial S_e} = -(-(\mu + \alpha_e\lambda_e)p_4 + \alpha_e\lambda_e p_5) \\
&= (\mu + \alpha_e\lambda_e)p_4 - \alpha_e\lambda_e p_5, \\
\dot{p}_5 &= -\frac{\partial H}{\partial I_e} = -\big(c_2 - p_4\alpha_e\beta_e + p_5\alpha_e\beta_e \\
&\quad - (\mu + \eta_e + \omega_e)p_5 - u_2 p_5 + (\eta_e + u_2)p_6\big) \\
&= -c_2 + (p_4 - p_5)\alpha_e\beta_e \\
&\quad + (\mu + \eta_e + \omega_e)p_5 + u_2 p_5 - (\eta_e + u_2)p_6, \\
\dot{p}_6 &= -\frac{\partial H}{\partial R_e} = -(\gamma_e p_4 - (\mu + \gamma_e)p_6) = -\gamma_e p_4 + (\mu + \gamma_e)p_6,
\end{aligned} \tag{6}$$

with the transversality conditions:

$$\begin{aligned} p_1(t_f) = 0,\ p_2(t_f) = 0,\ p_3(t_f) = 0, \\ p_4(t_f) = 0,\ p_5(t_f) = 0,\ p_6(t_f) = 0. \end{aligned} \tag{7}$$

Next, the function reaches its optimum when $\frac{\partial H}{\partial u_1} = 0$ and $\frac{\partial H}{\partial u_2} = 0$. It follows:

$$u_1 = \frac{(p_2 - p_1)\lambda_c S_c + (p_5 - p_4)\lambda_e S_e}{c_3},$$

$$u_2 = \frac{(p_2 - p_3)I_c + (p_5 - p_6)I_e}{c_4}.$$

Therefore, using the upper and lower constraints of the admissible control, we obtain u_1^* and u_2^* as follows

$$u_1^* = \begin{cases} 1, & u_1 \geq 1, \\ \dfrac{(p_2 - p_1)\lambda_c S_c + (p_5 - p_4)\lambda_e S_e}{c_3}, & 0 \leq u_1 \leq 1, \\ 0, & u_1 \leq 0. \end{cases}$$

and

$$u_2^* = \begin{cases} 1, & u_2 \geq 1, \\ \dfrac{(p_2 - p_3)I_c + (p_5 - p_6)I_e}{c_4}, & 0 \leq u_2 \leq 1, \\ 0, & u_2 \leq 0. \end{cases}$$

or

$$u_1^* = \min\left\{\max\left\{0, \frac{(p_2 - p_1)\lambda_c S_c + (p_5 - p_4)\lambda_e S_e}{c_3}\right\}, 1\right\},$$

and

$$u_2^* = \min\left\{\max\left\{0, \frac{(p_2 - p_3)I_c + (p_5 - p_6)I_e}{c_4}\right\}, 1\right\}. \tag{8}$$

■

3.8. *Numerical Simulation*

This section presents a numerical simulation of the optimal control model for pneumonia transmission among toddlers and the elderly. The simulation is based on the mathematical model discussed in the previous subsection, namely the optimal control system, the objective functional, the adjoint system, and the characterization of the optimal controls given in eq. (2), eq. (3), eq. (6), and eq. (8), respectively, together with the transversality conditions in eq. (7). The initial conditions are given by

$$\begin{aligned} S_c(0) = 0.99, \quad I_c(0) = 0.10, \quad R_c(0) = 0, \\ S_e(0) = 0.99, \quad I_e(0) = 0.10, \quad R_e(0) = 0. \end{aligned}$$

Using these initial conditions, the numerical solutions of the model without control and with the optimal control strategy are illustrated in Figure 1. Based on the epidemic model in eq. (1), the basic reproduction number is

$$R_0 = 5.69 > 1.$$

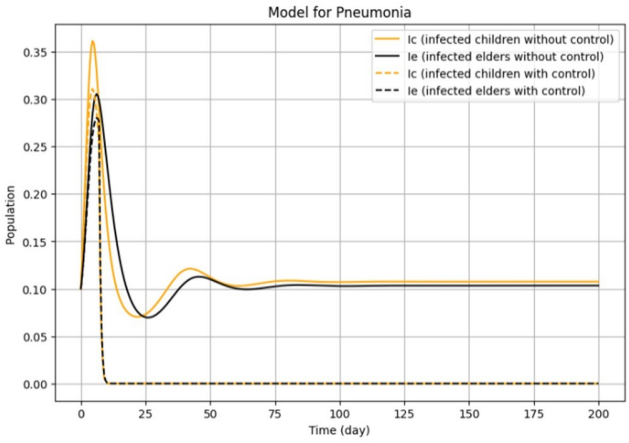

Figure 1. Infected children and the elderly individuals.

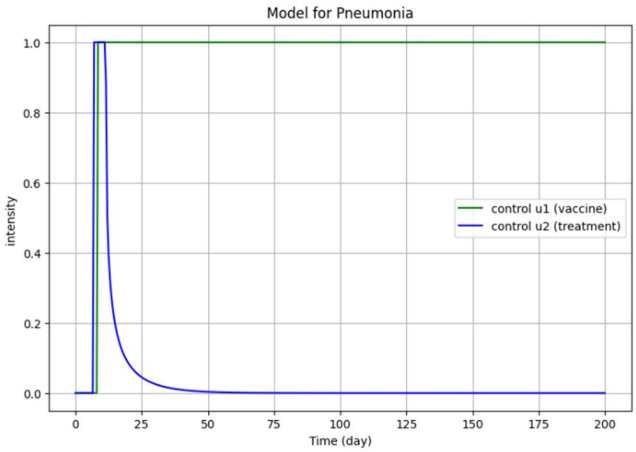

Figure 2. Control variables.

This result indicates that the disease persists in the population in the absence of intervention. The corresponding optimal control profiles are presented in Figure 2.

The simulation results presented in Figure 1 show that the infected populations of both children and the elderly in the absence of control are consistently higher than those under the optimal control strategy. Without intervention, both infected populations increase rapidly during the early stage of the epidemic, reaching their peak values before exhibiting damped oscillations and eventually converging to a positive endemic equilibrium. This behavior indicates that pneumonia persists in the population when no control measures are implemented.

In contrast, the implementation of the optimal control strategy substantially reduces the number of infected individuals in both age groups. The infected populations of children and the elderly decline rapidly after the intervention is introduced and approach zero within a relatively short period, indicating successful disease eradication. Moreover, the absence of oscillatory behavior in the controlled trajectories suggests that the intervention effectively stabilizes the system toward the disease-free equilibrium.

These results demonstrate that the combined implementation of vaccination and treatment strategies is highly effective in reducing disease prevalence among both children and the elderly. Compared with the uncontrolled scenario, the proposed inter-

vention not only suppresses the epidemic peak but also shortens the infectious period, thereby preventing the long-term persistence of the disease. Hence, the numerical simulations support the theoretical analysis and confirm that integrated control measures provide an effective approach for mitigating pneumonia transmission among vulnerable age groups.

Figure 2 illustrates the time-dependent optimal control strategies for vaccination (u_1, green curve) and treatment (u_2, blue curve). The optimal vaccination control remains at its upper bound, namely $u_1 = 1$, throughout the entire simulation period, indicating that the maximum vaccination effort should be maintained continuously. This finding suggests that sustained vaccination is the most effective long-term intervention for reducing pneumonia transmission and preventing the replenishment of the susceptible population.

In contrast, the optimal treatment control, u_2, exhibits a different pattern. The treatment effort rapidly increases to its maximum level during the early stage of the epidemic, reflecting the urgent need to immediately treat infected individuals and suppress disease transmission. After reaching its peak, the treatment intensity gradually decreases and eventually approaches zero as the epidemic progresses. This declining trend indicates that, once the number of infected individuals has been substantially reduced, intensive treatment is no longer economically optimal because the marginal benefit of additional treatment diminishes while the associated intervention costs remain.

Overall, the optimal control profiles indicate that vaccination should be implemented continuously throughout the intervention period, whereas treatment should be concentrated during the initial stage of the outbreak. This combination minimizes the disease burden while balancing the costs associated with the control measures. The results highlight the complementary roles of vaccination as a preventive strategy and treatment as a short-term mitigation strategy, demonstrating that early intensive treatment coupled with sustained vaccination provides the most effective approach for controlling pneumonia transmission.

Furthermore, to investigate the effect of increasing intervention costs, an additional simulation is performed by increasing both the vaccination and treatment costs by 10%. The corresponding simulation results are presented in Figure 3 and 4.

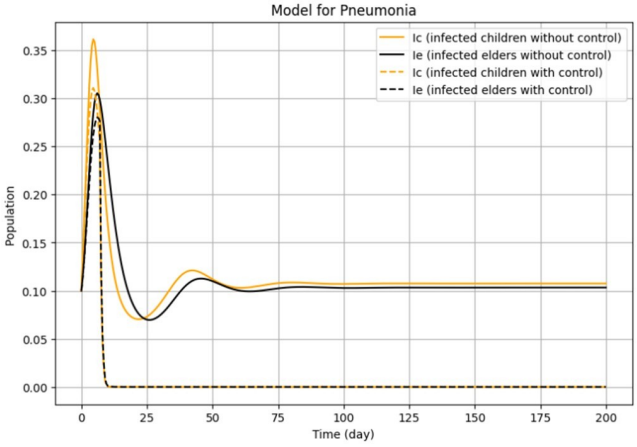

Figure 3. Infected children and the elderly individuals with increased intervention costs.

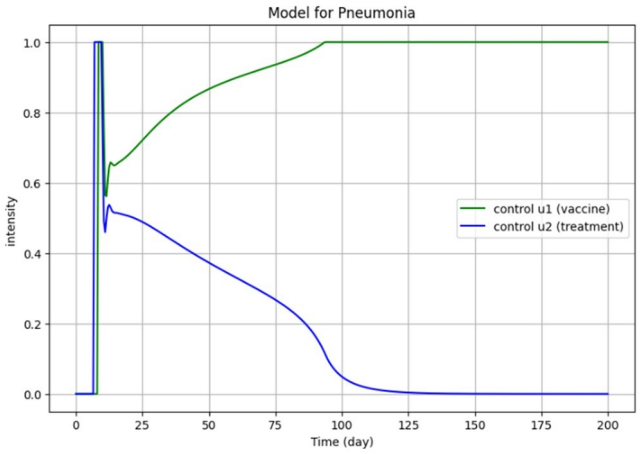

Figure 4. Control variables with increased intervention costs.

Figure 3 illustrates the dynamics of the infected populations among children and the elderly with and without optimal control, whereas Figure 4 presents the corresponding optimal vaccination and treatment control profiles. Compared with the baseline scenario, the infected populations, particularly among children, exhibit a slightly higher epidemic peak and require a longer time to reach equilibrium. A similar pattern is observed for the elderly population, although with a lower infection level. These results indicate that a 10% increase in both vaccination and treatment costs reduces the effectiveness of the intervention strategy, resulting in a greater disease burden before the system stabilizes. Nevertheless, the epidemic remains controllable through an appropriate combination of vaccination and treatment, albeit at a higher overall intervention cost.

Under the scenario of a 10% increase in vaccination and treatment costs, the optimal control strategy changes noticeably. As shown in Figure 4, the vaccination control, u_1, is maintained at a high level throughout the intervention period and gradually reaches its maximum intensity, indicating that sustained vaccination remains the most cost-effective strategy despite the increased implementation cost. In contrast, the treatment control, u_2, is applied intensively during the initial stage of the epidemic to rapidly reduce the number of infectious individuals. Subsequently, its intensity gradually decreases and eventually approaches zero as the epidemic progresses. This behavior reflects the higher treatment cost, making prolonged treatment less economically efficient.

Overall, these results suggest that increases in intervention costs substantially influence the optimal allocation of control efforts. Although the epidemic can still be effectively mitigated, higher vaccination and treatment costs require a more selective and economically balanced intervention strategy. This finding highlights the importance of maintaining affordable vaccination and treatment programs to ensure the long-term effectiveness of public health interventions for pneumonia control.

To further evaluate the individual contribution of each intervention, additional simulations were performed by considering vaccination and treatment as single control strategies. The corresponding population dynamics are presented in Figure 5 and 6, while the associated optimal control profiles are shown

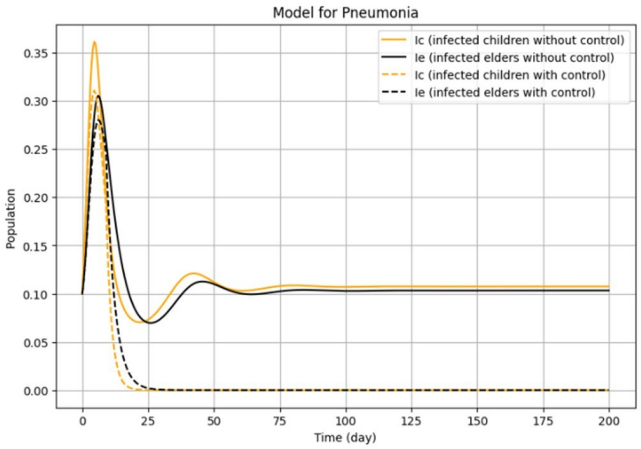

Figure 5. Infected children and the elderly individuals (with control vaccine only).

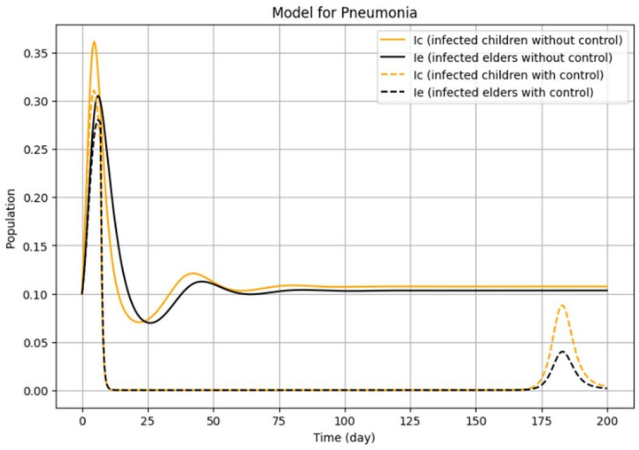

Figure 6. Infected children and the elderly individuals (with control treatment only).

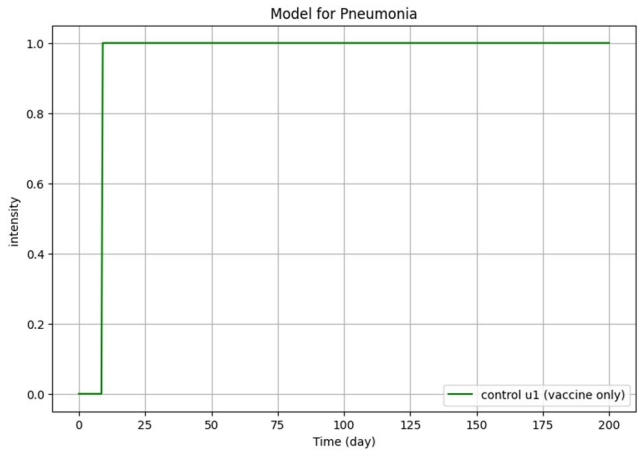

Figure 7. Control variable of vaccine only.

in Figure 7 and 8.

When vaccination is implemented as the sole intervention (Figure 5 and 7), the optimal vaccination control, u_1, remains at its maximum level throughout the simulation period. This strategy effectively suppresses disease transmission by reducing the number of susceptible individuals entering the infectious class.

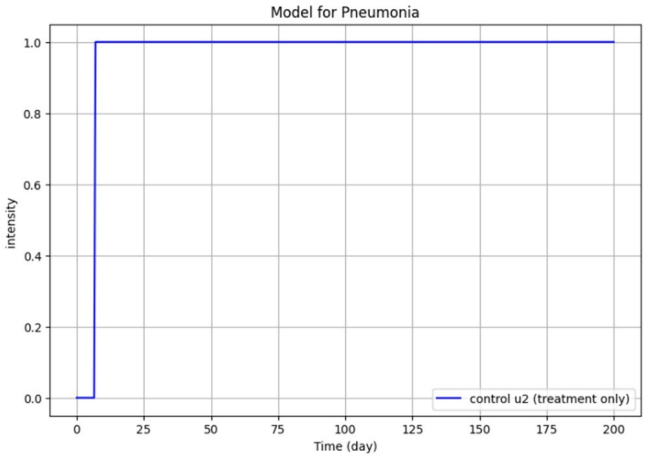

Figure 8. Control variable of treatment only.

Consequently, the infected populations of both children and the elderly decline rapidly following the initial outbreak and gradually converge to a stable endemic level without exhibiting significant secondary outbreaks.

In contrast, when treatment is applied as the only intervention (Figure 6 and 8), the optimal treatment control, u_2, is likewise maintained at its maximum intensity. Although this strategy initially reduces the number of infectious individuals, it is less effective in preventing subsequent disease transmission because treatment acts only after infection has occurred. As a result, a noticeable resurgence of the infected elderly population is observed toward the end of the simulation period, indicating that treatment alone is insufficient to completely suppress disease transmission.

Overall, the comparison demonstrates that vaccination provides greater long-term effectiveness than treatment when each intervention is implemented independently. Vaccination directly interrupts disease transmission by preventing new infections, whereas treatment primarily shortens the infectious period without eliminating the possibility of future transmission. These findings emphasize that preventive interventions have a greater impact on controlling pneumonia transmission than therapeutic interventions alone, while the combined implementation of vaccination and treatment remains the most effective strategy for minimizing the disease burden.

In summary, the numerical simulation results indicate that intervention strategies involving both vaccination and treatment for children and elderly individuals effectively reduce the infected populations. These findings provide useful insights for the development of public health policies and medical intervention programs, while also supporting previous studies on the transmission dynamics of pneumonia. Furthermore, future research should consider extending the proposed model by incorporating memory effects and fractional-order dynamics, as discussed in [20–23].

4. Conclusion

The mathematical model for the spread of pneumonia in children and the elderly is developed by adding control variabels for vaccines and treatment to the child and elderly populations. The model obtained is an optimal control model in the form of

a nonlinear differential equation system. The model was then solved using Pontryagin's Minimum Principle. Numerical simulation results show that with the application of controls in the form of vaccines and treatment for children and the elderly, the number of infected individuals is lower compared to the model without controls. In this case, Λ, β_c, and α_c are the most sensitive parameter from sensitivity analysis. Further research can be conducted by altering the assumptions regarding vaccine controls for children and the elderly. Changes to parameters or initial values can also be made to observe the dynamics of the model's solutions. In addition, it is essential to examine models that incorporate memory effects as well as fractional-order dynamics.

Author Contributions. **Dwi Lestari**: Conceptualization, methodology, software, validation, formal analysis, data curation, writing—original draft preparation, writing—review and editing, funding acquisition. **Nikenasih Binatari**: Conceptualization, validation, formal analysis, writing—review and editing, project administration, funding acquisition. **Eminugroho Ratna Sari**: Conceptualization, validation, formal analysis, writing—review and editing, project administration, funding acquisition.

Acknowledgement and Funding. The authors thanks for the the financial support to Department of Mathematics Education, Universitas Negeri Yogyakarta (UNY) and DRPM UNY for the Research Grant UNY 2025 under grant no. T/135/UN34.13/PT.01.03/2025.

Conflict of interest. The authors declare no conflicts of interest relevant to this article.

Data availability. Not applicable.

References

[1] R. Izadnegahdar, A. L. Cohen, K. P. Klugman, and S. A. Qazi, "Childhood pneumonia in developing countries," *The Lancet Respiratory Medicine*, vol. 1, no. 7, pp. 574–584, September 2013, doi:10.1016/S2213-2600(13)70075-4.

[2] Kementerian Kesehatan Republik Indonesia, "Pneumonia," apr 2025, [Online]. Available: https://ayosehat.kemkes.go.id/topik-penyakit/pencegahan-infeksi-bagi-bayi-dan-balita/pneumonia, [Accessed: 10-Februari-2025].

[3] D. W. Bahaye, T. Marijani, and G. Mlay, "An age-structured differential equations model for transmission dynamics of pneumonia with treatment and nutrition intervention," *Healthcare Analytics*, vol. 4, p. 100279, 2023, doi:10.1016/j.health.2023.100279.

[4] D. Aldila, N. Awdinda, Fatmawati, F. F. Herdicho, M. Z. Ndii, and C. W. Chukwu, "Optimal control of pneumonia transmission model with seasonal factor: Learning from jakarta incidence data," *Heliyon*, vol. 9, no. 7, p. e18096, July 2023, doi:10.1016/j.heliyon.2023.e18096.

[5] World Health Organization, "Pneumonia," nov 2021, [Online]. Available: http://www.who.int/news-room/fact-sheets/detail/pneumonia, note = [Accessed: 07-Februari-2025].

[6] United Nations Children's Fund, "Pneumonia," jul 2022, [Online]. Available: https://data.unicef.org/topic/child-health/pneumonia, [Accessed: 07-Februari-2025].

[7] Dinas Kesehatan Provinsi DKI Jakarta, "Laporan Rekapitulasi Penderita Berbasis Rumah Sakit," 2021, [Online]. Available: https://surveilans-dinkesdki.net/, [Accessed: 07-Februari-2025].

[8] Dinas Kesehatan Daerah Istimewa Yogyakarta, *Profil Kesehatan Diy Tahun 2018-2024*. Yogyakarta: Dinkes DIY, 2025.

[9] L. Dunn, "Pneumonia: Classification, diagnosis and nursing management," *Nursing Standard*, vol. 19, no. 42, pp. 50–54, June 2005, doi:10.7748/ns2005.06.19.42.50.c3901.

[10] N. MacDonald, E. Mohsni, Y. Al-Mazrou, J. Kim Andrus, N. Arora, S. Elden, M.-Y. Madrid, R. Martin, A. Mahmoud Mustafa, H. Rees, D. Salisbury, Q. Zhao, I. Jones, C. A. Steffen, J. Hombach, K. L. O'Brien, and A. Cravioto, "Global vaccine action plan lessons learned i: Recommendations for the next decade," *Vaccine*, vol. 38, no. 33, pp. 5364–5371, 2020, doi:10.1016/j.vaccine.2020.05.003.

[11] O. Ruuskanen, E. Lahti, L. C. Jennings, and D. R. Murdoch, "Viral pneumonia," *The Lancet*, vol. 377, no. 9773, pp. 1264–1275, April 2011, doi:10.1016/S0140-6736(10)61459-6.

[12] Shyamsunder, S. D. Purohit, and D. L. Suthar, "A novel investigation of the influence of vaccination on pneumonia disease," *International Journal of Biomathematics*, vol. 19, no. 04, p. 2450080, 2026, doi:10.1142/S1793524524500803.

[13] O. J. Otieno, M. Joseph, and O. Paul, "Mathematical Model for Pneumonia Dynamics with Carriers," *International Journal of Mathematical Analysis*, vol. 7, no. 49-52, pp. 2457–2473, 2013, doi:10.12988/ijma.2013.35109.

[14] T. L. Tirfe, L. L. Obsu, E. D. Gurmu, A. B. Celestine, and Shyamsunder, "Optimal control and bifurcation analysis of cholera model," *Journal of Prime Research in Mathematics*, vol. 2026, pp. 1–28, 2026.

[15] F. Brauer, "Backward bifurcations in simple vaccination models," *Journal of Mathematical Analysis and Applications*, vol. 298, no. 2, pp. 418–431, 2004, doi:10.1016/j.jmaa.2004.05.045.

[16] E. R. Sari, N. P. Puspita, and R. N. Farah, "Prevention of dengue virus transmission: insights from host-vector mathematical model," *Mathematical Modelling and Control*, vol. 5, no. 2, pp. 131–146, 2025, doi:10.3934/mmc.2025010.

[17] W. E. Boyce, R. C. DiPrima, and D. B. Meade, *Elementary Differential Equations and Boundary Value Problems*, 12th ed. John Wiley & Sons, 2021.

[18] R. U. Hurint, M. Z. Ndii, and L. Maria, "Analisis sensitivitas model epidemi SEIR," *Online Journal of Natural Sciences*, vol. 6, no. 1, pp. 22–28, 2017, doi:10.22487/25411969.2017.V6.I1.8076.

[19] L. Hakim and L. Widayanti, "Boundedness and existence analysis solution of an optimal control problem on mathematical COVID-19 model," *Barekeng: Jurnal Ilmu Matematika dan Terapan*, vol. 18, no. 2, pp. 0797–0808, 2024, doi:10.30598/barekengvol18iss2pp0797-0808.

[20] Shyamsunder and S. Purohit, "A novel study of the impact of vaccination on pneumonia via fractional approach," *Partial Differential Equations in Applied Mathematics*, vol. 10, p. 100698, 2024, doi:10.1016/j.padiff.2024.100698.

[21] E. Jalija, J. Amos, W. Atokolo, E. Abah, A. B. Celestine, G. O. Acheneje, Shyamsunder, and B. Bolaji, "Numerical solution of fractional order typhoid fever model via the generalized fractional adams-bashforth-moulton approach," *Network Modeling Analysis in Health Informatics and Bioinformatics*, vol. 15, no. 1, p. 68, February 2026, doi:10.1007/s13721-026-00743-1.

[22] K. Soni, Shyamsunder, and A. K. Sinha, "Memory-driven dynamics of hepatitis b transmission incorporating media awareness," *Advanced Theory and Simulations*, vol. 9, no. 5, p. e70394, 2026, doi:10.1002/adts.70394.

[23] T. D. Keno, O. D. Makinde, and L. L. Obsu, "Optimal control and cost-effectiveness analysis of pneumonia dynamics under the influence of environmental temperature change," *Network Modeling Analysis in Health Informatics and Bioinformatics*, vol. 14, no. 1, p. 16, December 2025, doi:10.1186/s12982-025-01316-9.